Biosensors and Bioelectronics 59 (2014) 321–327

Contents lists available at ScienceDirect

Biosensors and Bioelectronics

journal homepage: www.elsevier.com/locate/bios

A regeneratable, label-free, localized surface plasmon resonance (LSPR) aptasensor for the detection of ochratoxin A

Jin-Ho Park [a,1], Ju-Young Byun [a,1], Hyoyoung Mun [a], Won-Bo Shim [a], Yong-Beom Shin [c], Taihua Li [a], Min-Gon Kim [a,b,*]

[a] Department of Chemistry, School of Physics and Chemistry, Gwangju Institute of Science and Technology (GIST), 261 Cheomdan-gwagiro, Gwangju 500-712, Republic of Korea
[b] Advanced Photonics Research Institute, Gwangju Institute of Science and Technology (GIST), 261 Cheomdan-gwagiro, Gwangju 500-712, Republic of Korea
[c] Immune Therapy Research Center, Korea Research Institute of Bioscience & Biotechnology (KRIBB), 125 Gwahak-ro, Yuseong-gu, Daejeon 305-806, Republic of Korea

ARTICLE INFO

Article history:
Received 17 December 2013
Received in revised form
26 March 2014
Accepted 27 March 2014
Available online 12 April 2014

Keywords:
Localized surface plasmon resonance
Gold nanorod
Aptamer
Label-free detection
Ochratoxin A
Small molecule

ABSTRACT

Binding of an analyte on the surface of a nanoparticle typically promotes a change in the local refractive index, which gives rise to a shift in the wavelength of the localized surface plasmon resonance (LSPR) absorption band. The magnitude of the LSPR wavelength change is dependent on both the location of the analyte relative to the surface of the nanoparticle and the degree of alteration of the refractive index. We have employed this phenomenon as the basis for designing a new, label-free approach for the detection of the toxic mold mycotoxin, ochratoxin A (OTA) that employs a gold nanorod (GNR) and an aptamer target binding mechanism. In this system, binding of OTA causes an accumulation of OTA and G-quadruplex structure of the aptamer. This process results in a longitudinal wavelength shift of the LSPR peak associated with a change in the local refractive index near the GNR surface. By using this method, OTA can be quantitatively detected at concentrations lower than 1 nM. In addition, the results of this effort show that aptamer functionalized GNR substrate is robust in that it can be regenerated for reuse over seven times by heating in methanol at 70 °C to remove OTA. Moreover, the proposed biosensor system exhibits high selectivity for OTA over other mycotoxins. Finally, the sensor can be employed to detect OTA in ground corn samples with excellent recovery levels.

1. Introduction

Label-free assays that utilize localized surface plasmon resonance (LSPR) of noble metal nanoparticles has become widely used for detecting chemical and biological interaction due to rapid and simple to perform and less sensitive to temperature. (Lin et al., 2006; Balamurugan et al., 2013; Mayer and Hafner, 2011; Haes and Van Duyne, 2004). The reason for this is associated with the fact the frequencies of light that are resonant with the collective oscillation of electrons in metal nanoparticles (Sepulveda et al., 2009) are altered by refractive index changes of metal surfaces or colloidal aggregations promoted by the binding of molecules (Stewart et al., 2008). Specifically, an increase in refractive index at the surface of nanoparticles typically takes place when biomolecules are bound and this change leads to a red shift of the LSPR band. Importantly, the red shift of the LSPR band can be monitored easily by using scattering or absorption techniques. The LSPR band shift phenomenon has been employed in devising metal nanoparticle based sensors for detecting antigen/antibody (Endo et al., 2006; Mayer et al., 2008), biotin/streptavidin (Marinakos et al., 2007; Nath and Chilkoti, 2002; Nusz et al., 2008) and DNA interactions (Cao et al., 2005; Stoeva et al., 2005).

LSPR biosensors mainly fall in two classes depending upon whether they are colloidal or chip based. Most colloidal LSPR sensors are designed so that binding of an analyte causes particle aggregation to produce colloids. Commonly, these types of sensing systems rely on the analyte induced crosslinking of nanoparticles, which causes aggregate formation as a result of electronic dipole–dipole coupling between neighboring particles. Colloidal based LSPR sensing systems have been developed for the detection of environmental chemicals, toxins and biological agents (Vilela et al., 2012). In contrast, chip-based LSPR assay systems are formed by immobilization of colloidal metal nanoparticles (Huang et al. 2009a; Nath and Chilkoti, 2002; Truong et al., 2011) or metal nanostructure patterns on surfaces (Haes et al., 2004). The latter approaches have several advantages over aggregation based assay

* Corresponding author at: Advanced Photonics Research Institute, Gwangju Institute of Science and Technology (GIST), 261 Cheomdan-gwagiro, Gwangju 500-712, Republic of Korea. Tel.: +82 62 715 3330; fax: +82 62 715 2887.
E-mail address: mkim@gist.ac.kr (M.-G. Kim).
[1] Equally distributed in this work.

http://dx.doi.org/10.1016/j.bios.2014.03.059
0956-5663/

methods, including device miniaturization, regeneration and reuse, multiplex detection capabilities, applicability to single nanoparticle studies, and the ability to introduce a broad range of surface functionalities (Mayer and Hafner, 2011). However, to date, the targets of chip based LSPR biosensors have been large biomolecules such as protein or biopolymer (Endo et al., 2005; Anker et al., 2009; Deng et al., 2010; Akil-Jradi et al., 2011). Although having potential use in various areas such as food safety, environmental monitoring and metabolite analyses, label-free LSPR detection of small molecules remains a challenge because refractive index changes induced by these substances on nanoparticle surfaces are much smaller than those promoted by binding of large biomolecules.

In the study described below, a new, reliable, and direct LSPR aptamer based method for detecting an important small molecule was developed. The aptamer utilized in this system, which models those used as receptors in other biosensors, is comprised of a short sequence of single strand DNA that binds the target with a high affinity and specificity. The small molecular size of the aptamer enables it to undergo efficient immobilization to produce high density accumulation on the surface of the nanoparticle, a vitally important feature of all multiplexing miniaturized systems (*e.g.*, bioarrays or biochips). Furthermore, the new aptamer-based biosensor system has the advantage of reusability, which is not shared by antibody based sensors. Because it takes place close to the nanoparticle surface and it leads to stabilization through formation of a G-quadruplex structure, (Chiu and Huang, 2009; Yang et al., 2011) interaction of the nanoparticle linked aptamer with the target molecule is expected to generate an enhanced LSPR wavelength shift compared with those stimulated by antibody–antigen interactions in antibody based LSPR sensors. Furthermore, the conformational change undergone by the aptamer should results in an increase in density of receptor layer and a decrease in its thickness, factors that should contribute to a high sensitivity for target molecule detection.

The feasibility of the LSPR aptamer based strategy was demonstrated by employing it to develop a biosensor for the detection of ochratoxin A (OTA), a mycotoxin produced by molds whose toxicity represents a serious hazard to human and animal health. Therefore, methods for sensitive and rapid detection of OTA are exceptionally important for food safety, environmental monitoring, and quality control purposes (Zollner and Mayer-Helm, 2006). However, methods devised to date for OTA detection rely on expensive instrumentation and require time-consuming, complex sample preparation procedures (Ahn et al., 2012; Cuccioloni et al., 2008; Huang et al., 2010, Shim et al., 2007). As compared to those methods based on toxin-specific antibody, biosensors based on aptamer specific for OTA are highly flexible. Although several papers have reported the detection of OTA by utilizing aptamer, those procedures and modification steps are still not simple, which always need more than one DNA probe and more expensive labeling. In the current investigation we have developed a simply operated, cost-effective and rapid OTA monitoring system, which employs direct LSPR detection of binding of the target to an aptamer immobilized on the surfaces of gold nanorods (GNR). The LSPR sensor contains a 43 mer OTA aptamer with a thiol group at the 5′ end, which serves as an anchor to the gold surface. This aptamer, immobilized on the GNR surface via a thiol–gold linkage, self-assembles into a G-quadruplex structure upon interaction with OTA. The geometric change associated with formation of the G-quardruplex structure induces a red shift of the LSPR peak as a consequence of a refractive index change occurring at the GNR surface (Scheme 1b). Owing to the noncovalent, reversible nature

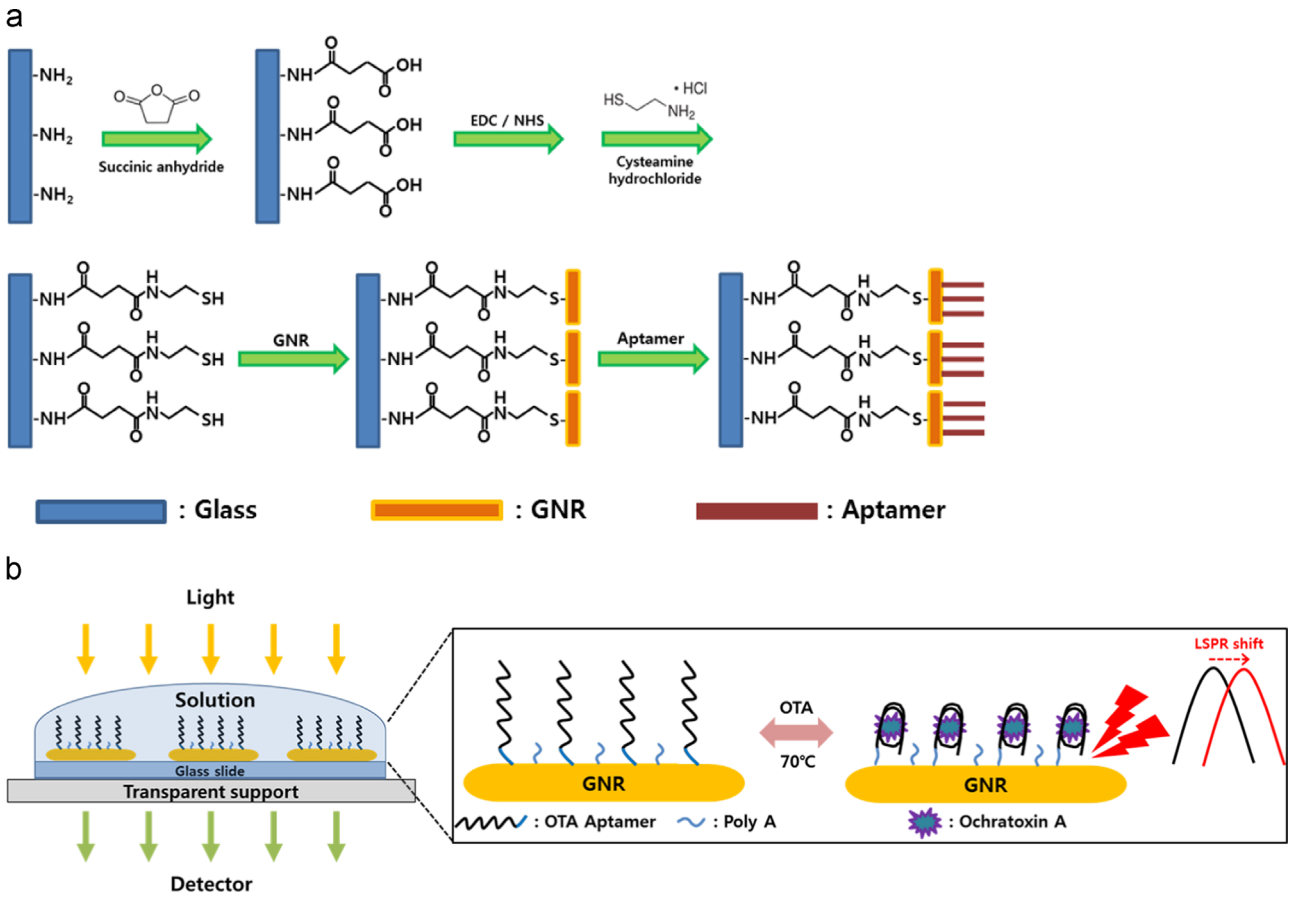

Scheme 1. Schematic illustration of (a) the fabrication procedure of OTA sensing substrate and (b) label-free OTA sensing system using a GNR based regenerable aptasensor.

of the interaction between OTA and the bound aptamer, the assay system can be regenerated after use by heating in methanol at 70 °C. In this work we have studied, for the first time, the chip-based LSPR aptasensor to detect and quantify small molecular compounds such as OTA with label-free manner, taking advantage of structure change of aptamer.

2. Experimental methods

2.1. Reagents

Sodium borohydrate ($NaBH_4$), gold(III) chloride trihydrate ($HAuCl_4$), silver nitrate ($AgNO_3$), L-ascorbic acid, cetyltrimethylammonium bromide (CTAB), succinic anhydride, (3-aminopropyl)trimethoxysilane (APTMS), cysteamine hydrochloride, *N*,*N*-dimethylformamide (DMF), potassium chloride (KCl), tris(2-carboxyethyl) phosphine hydrochloride (TCEP), *N*-ethyl-*N*′-(3-dimethylaminopropyl) carbodiimide hydrochloride (EDC), *N*-hydroxysuccinimide (NHS), ochratoxin A (OTA), aflatoxin B1 (AFB1) and zearalenone (ZEA) were purchased from Sigma-Aldrich (Milwaukee, WI, USA). OTA aptamer (5′-HS-AAAAAAA-AAAGCATCTGATCGGGTGTGGGTGGCGTAAAGGAAA) and Poly A (5′-HS-AAAAAAAAAA) were obtained from XENOTECH in Korea. The OTA aptamer sequence is identical with that reported in the literature (Cruz-Aguado and Penner, 2008).

2.2. Synthesis of gold nanorod

Gold nanorods (GNRs) were synthesized using a seed-mediated method (Nikoobakht and El-Sayed, 2003; Liu and Guyot-Sionnest, 2005). A seed solution was prepared by adding 3 mL of 0.01 M $NaBH_4$ to mixture of 3.75 mL of 0.1 M CTAB and 0.125 mL of 0.01 M $HAuCl_4$. Immediately, $NaBH_4$ was added to the mixture, followed by vigorous stirring for 2 min and standing at 25 °C. The growth solution was prepared by mixing slowly 33.04 mL of 0.1 M CTAB, 1.4 mL of 0.01 M $HAuCl_4$ and 0.21 mL of 0.01 M $AgNO_3$. The bright brown–yellow color of the solution disappeared upon addition of 0.21 mL of 0.1 M ascorbic acid. The growth solution was mixed with 0.14 mL of seed solution and allowed to stand for 3 h. The UV/vis absorption spectrum of the GNR solution was obtained by using a 96 well plate reader (Infinite M200pro, TECAN Group, Ltd., Switzerland). The size and aspect ratio were determined by using high resolution transmission electron microscopy (HR-TEM, JEM-2100, JEOL Ltd., Japan).

2.3. Fabrication of GNR substrate

The GNR substrate was fabricated as previously described report (Byun et al., 2013). The fabrication method of GNR substrate is illustrated in Scheme 1a. Glass slides (10 mm × 10 mm × 2 mm) were cleaned in piranha solution at 65 °C for 30 min. In order to generate the amine surface, the slide was rinsed with ethanol and immersed in an ethanolic 2% APTMS solution at room temperature for 1 h. The amine modified slide was subjected to 1 M succinic anhydride in DMF at 37 °C for 12 h, and then washed with DW and dried. A coupling reaction between the carboxylate groups on the surface and the amine groups was promoted treating the slide with a solution of 100 mM EDC and 25 mM NHS in DW for 15 min, followed by immersion in 100 mM cysteamin in DW. Finally, in order to prepare the GNR substrate the thiol-modified glass slide was exposed to the GNR solution for over 20 h. Before immobilization of the GNR on the glass slide, CTAB of GNR was removed by centrifugation three times at 10,000 rpm for 15 min each. The presence of immobilized GNRs on the glass slide was confirmed using field emission scanning electron microscopy (FE-SEM, S-4700, Hitachi Ltd., Japan).

2.4. OTA—Aptamer binding process

The disulfide bonds of the aptamer in a mixture (1:1 (v/v)) of OTA aptamer and poly A was cleaved by treatment with 5 mM TCEP. The mixture containing the aptamer in its free thiol form was exposed to the GNR substrate in 10 mM acetate buffer (pH 5.0) for 24 h. OTA at specific concentrations was added to the aptamer-anchored GNR substrate along with binding buffer (10 mM KCl in 0.1 M Tris–HCl, pH 7.2). Incubation for 20 min at 25 °C was followed by LSPR measurements. To regenerate the aptasensor after each cycle of OTA detection, the OTA bound chip was incubated in 10% methanol at 70 °C for 20 min and then was rinsed with binding buffer. OTA at diverse concentrations was then re-added to the regenerated aptamer GNR substrate followed by incubation and LSPR measurements at 25 °C.

2.5. Measurement and experimental set up

The end side of aptamer-modified GNR substrates was fixed on transparent 96 well plate cover using double-sided adhesive tape. A 200 μL of binding buffer was loaded on GNR substrate afterward OTA was added. After 20 min, washed GNR substrate with binding buffer was inserted into the 96 well plate reader (Infinite M2000pro, TECAN Group, Ltd., Switzerland) and measured with absorbance scan mode. In every measurement, a volume of solution on GNR substrate was adjusted to 200 μL. GNR substrate was scanned from 500 nm to 900 nm wavelength range with 10 times flash. The temperature was automatically maintained at 25 °C by equipment with 0.1 °C resolution. All the LSPR spectra were fitted by using the origin 7.5 program prior to calculation of $\Delta\lambda_{max}$ values. The measured LSPR spectra were fitted with smoothing and interpolation process. In this study, five times more wavelength intervals than raw LSPR spectra were obtained by using the interpolation procedure.

2.6. Spiking test

A spiked sample was generated from OTA contaminated ground corn powder. A 2% NaCl in 30% methanol solution containing 1 μM of OTA was added to 1 g of ground corn powder with. The mixture was shaken vigorously for 15 min and centrifuged at 4000 rpm for 15 min. The supernatant was separated and filtered by using a syringe filter with a 0.2 μm size pore. The filtrate was then analyzed either directly or after dilution using the aptamer-anchored GNR substrate system.

3. Results and discussion

3.1. Characterization of GNRs and the fabricated GNR substrate

The TEM image (Fig. S1a) of GNRs, synthesized GNRs by using the seed-mediated method, shows that they possess size uniformity with an average aspect ratio of 3.04 (32.5 ± 3.13 nm length and 10.7 ± 1.62 nm width). The UV–vis absorption spectrum (Fig. S1c) of the colloidal GNRs contains two distinct maxima corresponding to a transverse plasmon band at 515.01 nm and a longitudinal plasmon band at 699.69 nm. Following immobilization on a glass slide, bands in the extinction spectrum of the GNR become red-shifted relative to those of the GNR colloid state. The red-shift is likely the consequence of the higher refractive index of the glass slide compared to that of water, although interparticle coupling may contribute to this phenomenon (Szunerits and Boukherroub, 2012; Huang et al., 2009b). Inspection of the SEM image (Fig. S1b) of the GNRs immobilized on a glass slide (GNR substrate) shows that the nanoparticles are randomly distributed on the surface and that they are aligned parallel to the substrate.

Although most are separated from one another, some of the GNRs exist in an aggregated state on the surface. This feature might contribute to the slightly broader nature but not the peak positions of the UV–vis absorption bands of the immobilized GNRs.

3.2. OTA analysis by GNR based LSPR aptasensor

A monolayer of the OTA aptamer, comprised of a specifically designed 43 mer with thiol groups at their 5′ ends, was formed on the GNR substrate by taking advantage of thiol–gold interactions. Following immobilization, a red shift of the LSPR peak of the GNR from 704.10 nm to 712.91 nm takes place. Addition of OTA (1 μM) to the aptamer coated GNR substrate causes an red shift of the LSPR band from 712.91 to 716.71 nm, indicating that OTA has become bound to the aptamer (Fig. 1a). The specificity of OTA induced LSPR peak shift was explored by comparing OTA promoted spectral changes of GNR surfaces coated with OTA-aptamer with one coated with poly A and a bare surface not containing the OTA-aptamer. The results show that the LSPR peak positions are minimally affected by treatment of a bare and poly A coated surface with OTA (Fig. 1b and c). This finding demonstrates that the bare GNR surface and one containing a self-assembled monolayer of poly A are unable to bind OTA. In the detection using LSPR, all the measured LSPR sepctra were fitted as discribed in the experimental methods section. The additional raw data can be found in the Supporting information (Fig. S2). The fitted data in each steps presented match well to those observed for raw data. In case of measuring the wavelength shift of LSPR peak, the λ_{max} values are measured by tracing peak position from the fitted spectra.

In order to gain furhter support for the conclusion that the LSPR shift is caused by OTA binding to the aptamer coated GNR substrate, a slide generated by application of OTA to the aptamer coated GNR substrate was washed, and then extracted by incubation in 10% methanol at 70 °C. The extracted solution was then analyzed by using fluorescence spectroscopy. The emission spectrum (excitation at ca. 380 nm) of the methanol extract contained a band with a maximum at ca. 440 nm (Fig. 1d, green-dotted line), which is same as that produced by a 1 μM solution of OTA (Fig. 1d, blue line) (Pohland et al., 1992). In addition, the methanol extract of both an OTA treated poly A coated GNR substrate and an OTA treated bare GNR substrate do not display significant fluorescent signals at 440 nm (Fig. 1d, red line and yellow line).

As is typically observed for aptamer target systems, OTA binding should promote a large change of the OTA-aptamer structure from a random and coiled conformation to a G-quartet or other compact structures. As a result of this phenomenon and the fact that it causes the distance between OTA and surface of GNR to become shorter, the refractive index associated with the local dielectric environment near the surface of GNR changes and results in a peak shift of the LSPR band. The LSPR spectral shift ($\Delta\lambda$) in response to changes in the refractive index of GNR surface is described by the equation, (Mayer and Hafner, 2011; Szunerits and Boukherroub, 2012).

$$\Delta\lambda = m\Delta n \exp(-2d_L/l_d)[1-\exp(-2d_A/l_d)],$$

where $\Delta\lambda$ is the LSPR shift, m is the refractive index sensitivity of the GNR, Δn is the change in the refractive index in reflective index units, the analyte thickness d_A, binding to the nanoparticle surface modified with a molecular recognition element of thickness d_L, and l_d is the sensing depth. Binding of the analyte takes place at a certain distance from the metal surface, determined by the dimensions of the recognition layer the analyte. Analysis of the equation shows that the LSPR shift is affected by a molecular

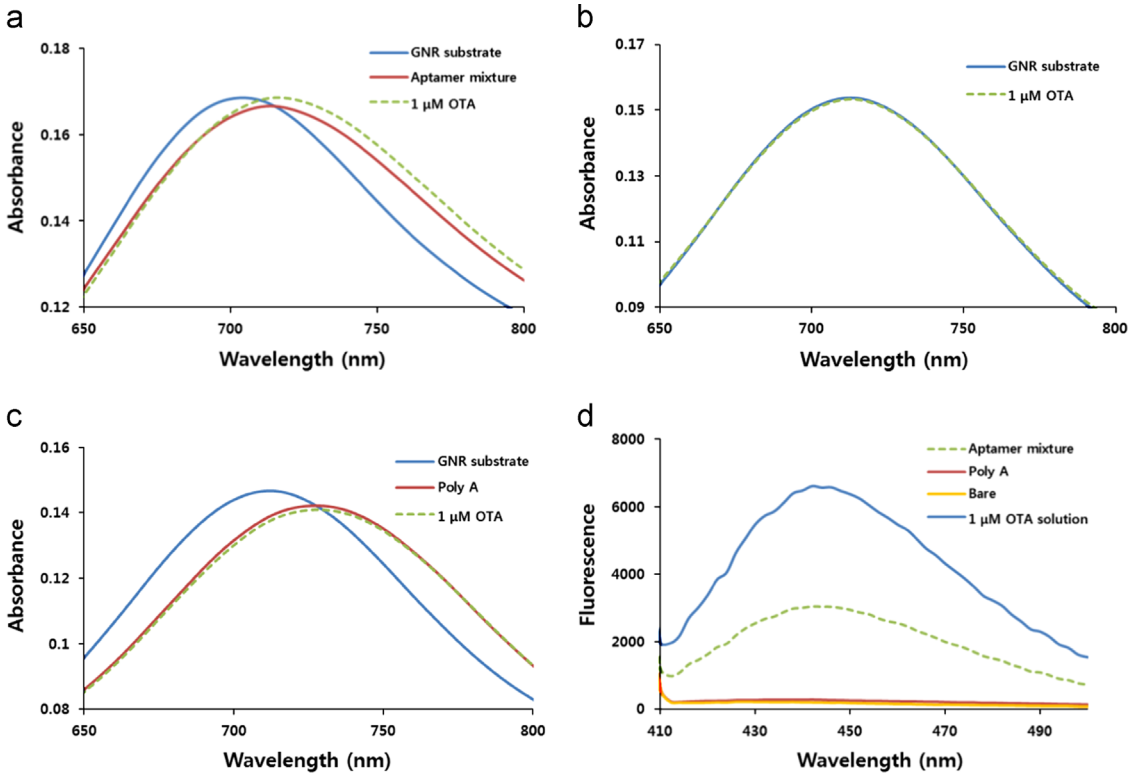

Fig. 1. (a) LSPR spectra of an aptasensor before and following OTA binding. The solid and dotted lines represent the peak wavelength shift before and after OTA binding at the surface of aptamer-GNR substrate, respectively. ((b) and (c)) The specificity of the OTA induced LSPR peak-shift was confirmed by replacing the OTA-aptamer with poly A (b) or without aptamer mixture (bare GNR surface) (c). (d) Fluorescence spectra of a 1 μM OTA solution (blue), a solution of OTA extracted from aptamer-GNR substrate (green), poly A-anchored GNR substrate (red), and bare GNR surface (yellow). Fluorescence spectra were recorded with excitation at 380 nm. (For interpretation of the references to color in this figure legend, the reader is referred to the web version of this article.)

recognition element thickness (receptor layer, d_L) and a change in the refractive index (Δn) if all other conditions are constant.

Attachment of the aptamer mixture (receptor layer) to the surface of the GNR causes a red shift in the LSPR peak as a consequence of a refractive index change from that of water ($RI = 1.33$) to that of the aptamer ($RI = 1.5–1.6$). Specific binding of OTA ($RI = 1.53$) to the immobilized OTA specific aptamer layer leads to a further red shift of the LSPR peak. Because most organic substances have higher refractive indicies than do buffer solutions (Anker et al., 2008), their binding to nanoparticle surfaces causes the local refractive index to increase and this accompanied by a red shift of the LSPR peak. A second factor affecting the LSPR red shift is the change in density of OTA-aptamer complex on the GNP surface brought about by transformation of the uncomplexed, random and coiled conformation to the G-quadruplex strucure. This phenomenon should lead to an increase in the density and a decrease in the thickness of the OTA aptamer complex conatining layer on the GNRs surface and, thus, a larger LSPR peak shift.

3.3. Sensitivity and selectivity

The response of the aptamer-GNR sensor system to OTA concentrations was evaluated. Incremental red shifts in the LSPR band were observed to take place when various concentrations of OTA in the range of 1 nM–1 μM were applied to the aptamer coated GNR substrate. The specific wavelength shifts, relative to that of the aptamer coated substrate at 713.31 nm, are 1.00 nm at 1 nM OTA, 1.80 nm at 10 nM OTA, 2.80 nm at 100 nM OTA and 3.60 nm at 1 μM OTA (Fig. 2a). The calibration plot in Fig. 2b displays the dependence of the LSPR shift on the concentration of OTA. The linear range for OTA detection was found to be from 0.1 nM to 10 μM with a relative correlation coefficient of 0.9732 and the sensitivity of OTA detection is reached to 1 nM (Fig. 2b).

The selectivity of the OTA sensing system was explored using aflatoxin b1 (AFB1) and zearaleone (ZEA), both of which are present in naturally contaminated grain samples. These mycotoxins have similar chemical groups such as benzene ring, hydroxyl and methyl group and small molecular weight under the 500 MW (Fig. S3). As the results are presented in Fig. 3, no significant LSPR peak shift occurs when AFB1 and ZEA are applied to the OTA-aptamer-GNR substrate. Moreover, the presence of these toxins does not interfer with the systems ability to sense OTA. The findings show that the new biosensor is selective for OTA in a manner that is not affected by the presence of other contaminating mycotoxins of similar molecular weight.

3.4. Regeneration of aptamer sensor

In general, aptamers can be denatured and refolded multiple times without loss of their activity. This property is partly a result

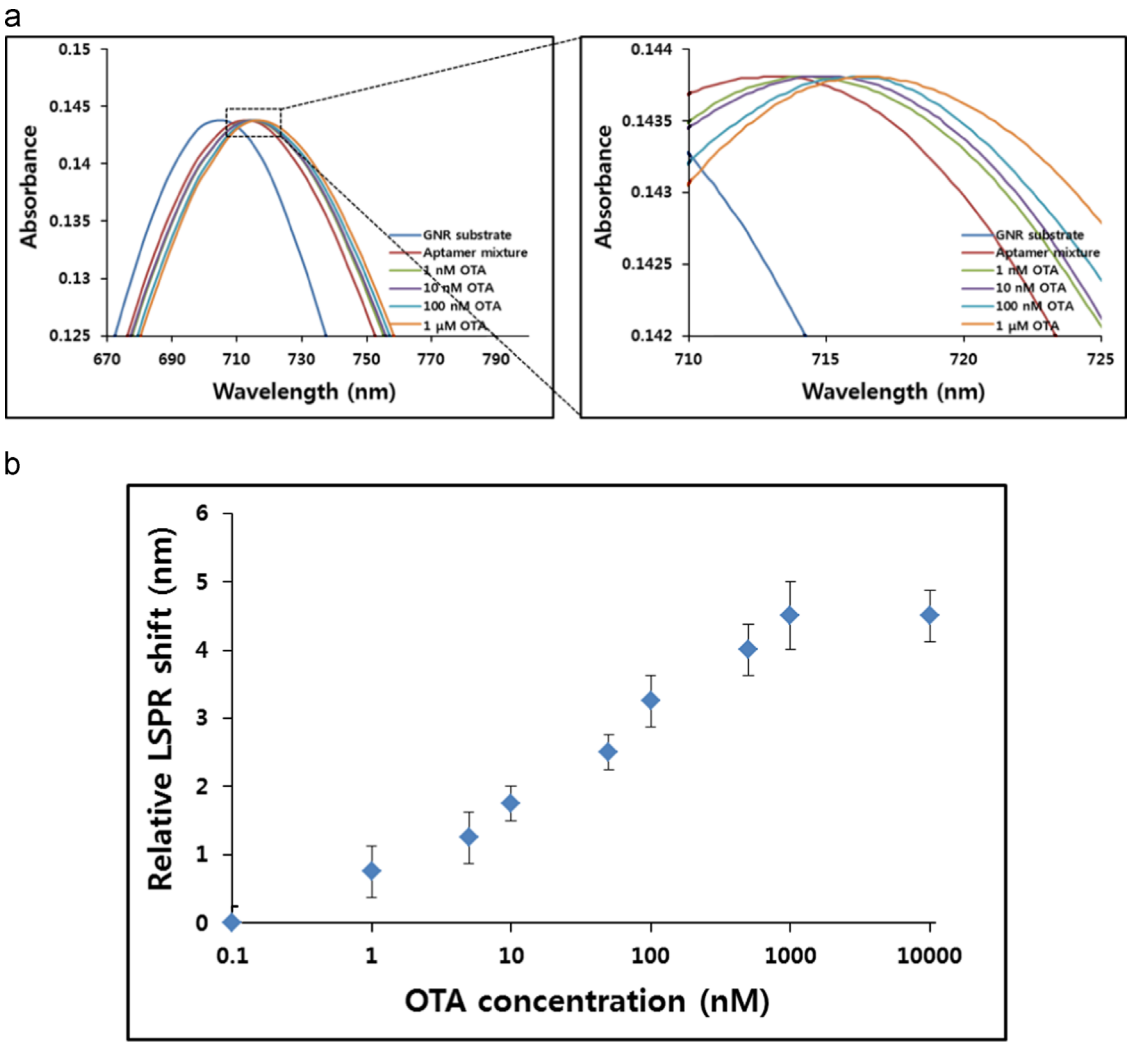

Fig. 2. (a) Normalized UV–vis adsorption spectra and (b) a response curve of LSPR peak shift of aptamer-GNR sensor on sequential incubation from 0.1 nM to 10 μM of OTA (GNR substrate: blue line, aptamer-GNR substrate: red line, 1 nM (green), 10 nM (violet), 100 nM (sky blue) and 1 μM (orange) OTA-loaded aptamer-GNR substrate). (For interpretation of the references to color in this figure legend, the reader is referred to the web version of this article.)

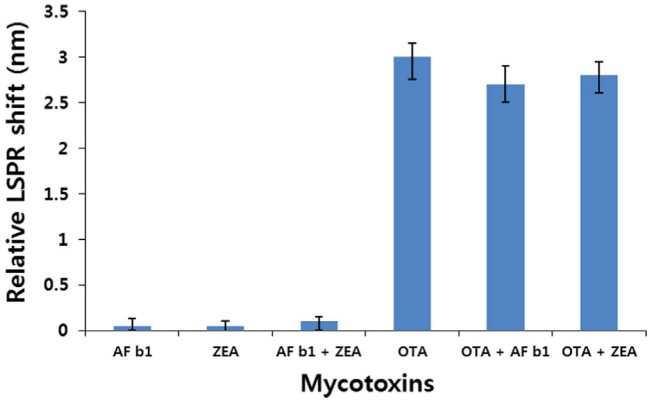

Fig. 3. The selectivity of the LSPR based aptasensor. The concentration of OTA was 100 nM, and those of the other non-target mycotoxins are 1 μM.

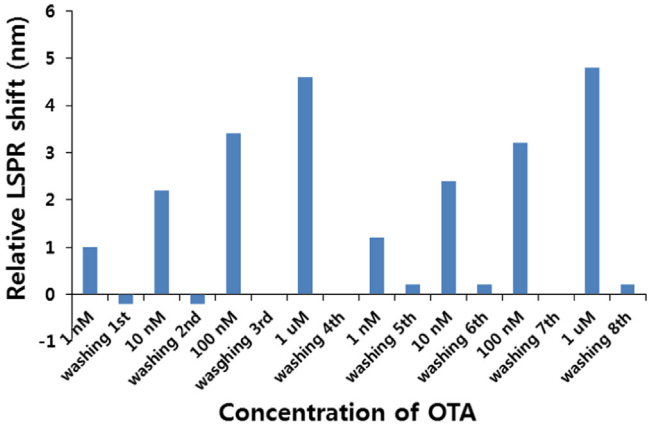

Fig. 4. Regenerable property of LSPR aptasensor. LSPR peak shifts following seven repeated regeneration—OTA binding cycles.

Table 1
Recovery of OTA in the spiked corn samples.

Spiked OTA Concentration (nM)	LSPR Shift (nm)	OTA Concentration (nM)	Recovery (%)
10	2.06	10.9	108.3
100	2.97	108.3	109.4

of the fact that the binding function of the aptamer is a consequence of multiple, simple, non-covalent interactions. Therefore, we reasoned that it should be possible to reuse the aptamer-GNR substrate system for LSPR based OTA detection. This possibility was examined by subjecting the sensor to repeated OTA detection cycles involving OTA binding and spectroscopic analysis, denaturization promoted OTA release, and OTA rebinding and spectroscopic analysis. Denaturization promoted OTA release after each cycle of detection was carried out by incubating the aptamer-GNR substrate in 10% methanol for 20 min at 70 °C and then rinsing with DW. Importantly, the LSPR peak shifts of the seven-times recycled sensors promoted by OTA in the concentration range of 1 nM–1 μM (Fig. 4) were similar to those observed using freshly prepared sensor systems.

3.5. *Application for OTA analysis in a real sample*

The potential applicability of the OTA sensing system to real time analysis was evaluated using spiked corn samples containing specific concentrations of OTA. The OTA-spiked corn samples were extracted with a 30% methanol solution containing 2% NaCl. The extracts were applied to aptamer-GNR substrates, which were then subjected to LSPR analysis. Inspection of the LSPR peak shift data (Table 1) arising from these experiments shows that the level of recovery of the respective 10 nM and 100 nM spiked corn samples were 108.3% and 109.4%.

4. Conclusions

In the investigation described above, we developed a label-free aptasensor based technique for quantitatively detecting the important mycotoxin, OTA. The system relies on red shifts of LSPR wavelengths that are promoted by binding of OTA to a OTA-aptamer coated GNR substrate. The wavelegth shifts are a consequence of the large changes that take place in the refractive index at the GNR surface caused by OTA binding induced aptamer folding to form a G-quadruplex structure. A linear response was observed for LSPR red shifts as a function of OTA concetrations. In addition, the lower limit of the system for OTA detection is below 1 nM. Importantly, the aptasensor system can be regenerated after use by employing a simple extraction method. Finally, the practical use of the sensing system was demosntrated by its application to the quantitative determination of OTA in spiked corn samples. In addition to leading to the developemnt of a simple, label free, highly sensitive and specific, and regeratable LSPR based OTA sensing system, this investigation has demonstrated a new strategy that can potential be employed to design other sensors for biologically relavent small molecules.

Acknowledgments

This work was financially supported by grants from the GRL Program (2013K1A1A2A02050616) and the NLRL Program (2011-0028915) through the National Research Foundation of Korea (NRF) funded by the Korean Ministry of Science, ICT & Future Planning, and this research was also supported by the Basic Science Research Program through the NRF funded by the Ministry of Education (NRF-2013R1A1A2009918).

Appendix A. Supporting information

Supplementary data associated with this article can be found in the online version at http://dx.doi.org/10.1016/j.bios.2014.03.059.

References

Anker, J.N., Paige Hall, W., Lambert, M.P., Velasco, P.T., Mrksich, M., Klein, W.L., Van Duyne, R.P., 2009. J. Phys. Chem. C 113, 5891–5894.
Akil-Jradi, S., Jradi, S., Plain, J., Bijeon, J., Sanchez, C., Bachelot, R., Royer, P., 2011. Chem. Commun. 47, 2444–2446.
Ahn, J.H., Jeong, Y.S., Lee, T.G., Kim, Y.P., Kim, H.S., 2012. Biochip J. 6, 34–40.
Anker, J.N., Paige Hall, W., Lyandres, O., Shah, N.C., Zhao, J., Van Duyne, R.P., 2008. Nat. Mater. 7, 442–453.
Balamurugan, S., Mayer, K.M., Lee, S., Scoper, S.A., Hafner, J.H., Spivak, D.A., 2013. J. Mol. Recognit. 26, 402–407.
Byun, J.Y., Shin, Y.B., Li, T., Park, J.H., Kim, D.M., Choi, D.H., Kim, M.G., 2013. Chem. Commun. 49, 9497–9499.
Cao, Y.C., Jin, R.C., Thaxton, S., Mirkin, C.A., 2005. Talanta 67, 449–455.
Chiu, T.C., Huang, C.C., 2009. Sensors 9, 10356–10388.
Cruz-Aguado, J.A., Penner, G., 2008. J. Agric. Food Chem. 56, 10456–10461.
Cuccioloni, M., Mozzicafreddo, M., Barocci, S., Ciuti, F., Pecorelli, I., Eleuteri, A.M., Spina, M., Fioretti, E., Angeletti, M., 2008. Anal. Chem. 80, 9250–9256.
Deng, J., Song, Y., Wang, Y., Di, J., 2010. Biosens. Bioelectron. 26, 615–619.
Endo, T., Kerman, K., Nagatani, N., Hiepa, H.M., Kim, D.K., Yonezawa, Y., Nakano, K., Tamiya, E., 2006. Anal. Chem. 78, 6465–6475.
Endo, T., Yamamura, S., Nagatani, N., Morita, Y., Takamura, Y., Tamiya, E., 2005. Sci. Technol. Adv. Mater. 6, 491–500.
Haes, A.J., Van Duyne, R.P., 2004. Expert Rev. Mol. Diagnost. 4, 527–537.

Haes, A.J., Zou, S., Schatz, G.C., Van Duyne, R.P., 2004. J. Phys. Chem. B 108, 6961–6968.
Huang, H., Tang, C., Zeng, Y., Yu, X., Liao, B., Xia, X., Yi, P., Chu, P.K., 2009a. Colloids Surf., B 71, 96–101.
Huang, B., Han, Z., Cai, Z., Wu, Y., Ren, Y., 2010. Anal. Chim. Acta 662, 62–68.
Huang, H., Tang, C., Zeng, Y., Yu, X., Liao, B., Xia, X., Yi, P., Chu, P.K., 2009b. Colloids Surf., B 71, 96–101.
Lin, H.-Y., Chen, C.-T., Chen, Y.-C., 2006. Anal. Chem. 78, 6873–6878.
Liu, M.Z., Guyot-Sionnest, P., 2005. J. Phys. Chem. B 109 (22192-19200).
Mayer, K.M., Lee, S., Liao, H., Rostro, B.C., Fuentes, A., Scully, P.T., Nehl, C.L., Hafner, J.H., 2008. ACS Nano 2, 687–692.
Marinakos, S.M., Chen, S., Chilkoti, A., 2007. Anal. Chem. 79, 5278–5283.
Mayer, K.M., Hafner, J.H., 2011. Chem. Rev. 111, 3828–3857.
Nath, N., Chilkoti, A., 2002. Anal. Chem. 74, 504–509.
Nusz, G.J., Marinakos, S.M., Curry, A.C., Dahlin, A., Hoeoek, F., Wax, A., Chilkoti, A., 2008. Anal. Chem. 80, 984–989.
Nath, N., Chilkoti, A., 2002. Anal. Chem. 74, 504–509.
Nikoobakht, B., El-Sayed, M.A., 2003. Chem. Mater. 15, 1957–1962.
Pohland, A.E., Nesheim, S., Friedman, L., 1992. Pure Appl. Chem. 64, 1029–1046.
Sepulveda, B., Angelome, P.C., Lechuga, L.M., Liz-Marzan, L.M., 2009. Nano Today 4, 244–251.
Stewart, M.E., Anderton, C.R., Thompson, L.B., Maria, J., Gray, S.K., Rogers, J.A., Nuzzo, R.G., 2008. Chem. Rev. 108, 494–521.
Stoeva, S.I., Huo, F.W., Lee, J.S., Mirkin, C.A., 2005. J. Am. Chem. Soc. 127, 15362–15363.
Shim, W.B., Yang, Z.Y., Kim, J.S., Kim, J.Y., Kang, S.J., Woo, G.J., Chung, Y.C., Eremin, S.A., Chung, D.H., 2007. J. Microbiol. Biotechnol. 17, 1629–1637.
Szunerits, S., Boukherroub, R., 2012. Chem. Commun. 48, 8999–9010.
Truong, P.L., Cao, C., Park, S., Kim, M., Sim, S.J., 2011. Lab Chip 11, 2591–2597.
Vilela, D., Gonzalez, M.C., Escarpa, A., 2012. Anal. Chim. Acta 751, 24–43.
Yang, C., Wang, Y., Marty, J.-L., Yang, X., 2011. Biosens. Bioelectron. 26, 2724–2727.
Zollner, P., Mayer-Helm, B., 2006. J. Chromatogr. A 1136, 123–169.